View metadata, citation and similar papers at core.ac.uk
brought to you by CORE
provided by Queensland University of Technology ePrints Archive

Raman Spectroscopy Of Beaverite And Plumbojarosite

Ray L. Frost•, Rachael-Anne Wills and Wayde Martens

This is the author-manuscript version of this paper. Published in:
Frost, Ray and Wills, Rachael and Martens, Wayde (2005) Raman spectroscopy of beaverite and plumbojarosite. *Journal of Raman Spectroscopy* 36(12): pp. 1106-1112.
Copyright 2005 Wiley.

Inorganic Materials Research Program, School of Physical and Chemical Sciences, Queensland University of Technology, GPO Box 2434, Brisbane Queensland 4001, Australia.

Abstract

Raman spectroscopy has been used to characterise the compound of formula $Pb(Fe^{3+},Cu^{2+})_3(SO_4)_2(OH)_6$ equivalent to synthetic beaverite, one of the jarosite subgroup minerals. The mineral is characterised by multiple OH stretching vibrations attributed to non-equivalent OH units in the structure. Multiple vibrations are observed for the SO_4^{2-} stretching vibrations indicating the non-equivalence of the sulphate units in the structure. This multiplicity is also reflected in the ν_2 and ν_4 bending modes. The Raman spectrum of beaverite is significantly different from that of plumbojarosite for which multiple bands are not observed.

Keywords: alunite, jarosite, plumboharosite, beaverite, Raman spectroscopy

Introduction

The mineral beaverite $[Pb(Fe,Cu)_3(SO_4)_2(OH)_6]$ is one mineral of the jarosite subgroup. [1] It was apparently first discovered in 1911. [2] Beaverite is like plumbojarosite in that it forms in close proximity to Fe-Pb-Cu sulphides. [1, 3] The mineral is related to jarosites and alunites and is trigonal. Beaverite forms a solid solution with plumbojarosite with replacement of the Fe^{3+} by Cu^{2+} or Zn^{2+} or both. [4] Lead jarosite also known as plumbojarosite ($PbFe_6(SO_4)_4(OH)_{12}$) was identified in relation to jarosite in 1902. [5] Plumbojarosite is often found in cationic mixed jarosites. [6-9] Such minerals are of importance in medieval and archaeological science [10,11] and are also found in mine drainage sites both ancient and modern [9,11,12]. Such formation of jarosites has been occurring since long before the Bronze Age. [13] The importance of jarosite formation and its decomposition depends upon its presence in soils, sediments and evaporate deposits. [14] These types of deposits have formed in acid soils where the pH is less than 3.0 pH units. [15] Such acidification results from the oxidation of pyrite which may be from bacterial action or through air-oxidation.

In many studies the assumption is made that synthetic jarosites are identical and behave the same as the natural jarosites. [16] Whilst some powder XRD studies can be used to study jarosites such studies are of limited value as the jarosite compounds may be poorly diffracting and the XRD pattern will be dominated by the highly

• Author to whom correspondence should be addressed (r.frost@qut.edu.au)

crystalline materials such as potassium sulphate which is present. Vibrational spectroscopy allows a better method for the study of these minerals. Infrared spectroscopy has been used to study jarosite minerals but failed to detect cationic differences in the jarosite structures. [17-22] Raman spectroscopy has been used to study jarosites but some previous studies failed to study the complete spectra. [18,19,23] It is doubtful if the vibrational spectroscopy of beaverite has ever been undertaken and certainly no comparison with the spectra of plumbojarosite has ever been made. Further the lack of crystallinity of the synthetic samples studied may have made the collection of Raman spectral data difficult. Most studies have involved the use of synthetic jarosites [16]. In this work, as part of our studies of secondary mineral formation, we report the Raman spectra of synthetic beaverite, relating the Raman spectra to the structure of beaverite and making a comparison with the Raman spectrum of plumbojarosite..

Experimental

Mineral

The mineral beaverite was synthesised according to the method given by Jambor and Dutrizac. [24] A 40mL chloride solution was prepared. It contained 0.25g $PbCl_2$, 5mL of 1.23M $FeCl_3$ and 12mL of saturated LiCl solution with the remaining volume being water. A separate sulphate solution was also prepared. This contained 2.5g $Fe_2(SO_4)_3$ and 4.62g $CuSO_4$ dissolved in a minimal volume of water. The sulphate solution was added dropwise to the chloride solution over a 5 minute time period. The solution was transferred to an autoclave and enough water was added to bring the final volume of the solution to approximately 0.1L. The autoclave was heated at 120°C for 3 days. After this time, the brown precipitate was collected, washed and dried under vacuum. 1.33g of sample was obtained and identified by X-Ray diffraction as beaverite. A model of beaverite is shown in Figure 1.

X-ray diffraction

X-Ray diffraction patterns were collected using a Philips X'pert wide angle X-Ray diffractometer, operating in step scan mode, with Cu K_α radiation (1.54052 Å). Patterns were collected in the range 3 to 90° 2θ with a step size of 0.02° and a rate of 30s per step. Samples were prepared as a finely pressed powder into aluminium sample holders. The Profile Fitting option of the software uses a model that employs twelve intrinsic parameters to describe the profile, the instrumental aberration and wavelength dependent contributions to the profile.

Raman spectroscopy

The crystals of beaverite or plumbojarosite were placed and oriented on the stage of an Olympus BHSM microscope, equipped with 10x and 50x objectives and part of a Renishaw 1000 Raman microscope system, which also includes a monochromator, a filter system and a Charge Coupled Device (CCD). Raman spectra were excited by a HeNe laser (633 nm) at a resolution of 2 cm^{-1} in the range between 100 and 4000 cm^{-1}. Repeated acquisition using the highest magnification was accumulated to improve the signal to noise ratio. Spectra were calibrated using the 520.5 cm^{-1} line of a silicon wafer. In order to ensure that the correct spectra are obtained, the incident excitation radiation was scrambled. Previous studies by the

authors provide more details of the experimental technique. Spectra at elevated temperatures were obtained using a Linkam thermal stage (Scientific Instruments Ltd, Waterfield, Surrey, England). Spectral manipulation such as baseline adjustment, smoothing and normalisation was performed using the GRAMS® software package (Galactic Industries Corporation, Salem, NH, USA).

Infrared spectroscopy

Infrared spectra were obtained using a Nicolet Nexus 870 FTIR spectrometer with a smart endurance single bounce diamond ATR cell. Spectra over the 4000–525 cm^{-1} range were obtained by the co-addition of 64 scans with a resolution of 4 cm^{-1} and a mirror velocity of 0.6329 cm/s. Spectra were co-added to improve the signal to noise ratio.

Spectroscopic manipulation such as baseline adjustment, smoothing and normalisation were performed using the Spectracalc software package GRAMS (Galactic Industries Corporation, NH, USA). Band component analysis was undertaken using the Jandel 'Peakfit' software package, which enabled the type of fitting, function to be selected and allows specific parameters to be fixed or varied accordingly. Band fitting was done using a Gauss-Lorentz cross-product function with the minimum number of component bands used for the fitting process. The Gauss-Lorentz ratio was maintained at values greater than 0.7 and fitting was undertaken until reproducible results were obtained with squared correlations of r^2 greater than 0.995.

In this experiment it should be noted that Raman spectra were obtained using a Renishaw Raman microscope and these spectra are compared with the infrared spectra obtained by using a single bounce diamond ATR cell. The Raman spectra are obtained from a sample size of 1 micron whereas the infrared spectra are collected from a sample size of at best 25 microns. The Raman spectra are thus obtained from a significantly smaller sample size. In the normal course of events Raman spectra are obtained from a number of crystals and from different positions on the same crystal. This ensures that typical mineral spectra are obtained. It should be noted that a comparison is being made between a microRaman spectrum which is orientation dependent with an infrared spectrum which is essentially from a bulk sample.

Results and discussion

X-ray diffraction

The powder X-ray diffraction pattern (PXRD) is shown in Figure 2. The reference XRD pattern for beaverite 47-1817 is also shown. The patterns are identical and no impurities within the limits of the PXRD method could be detected.

In the beaverite structure, there are three octrahedral sites connected to each SO_4 unit now if one lead site is replaced by Cu the symmetry is reduced to C_{2v} if two are replaced then C_s. There is no fundamental change just a change in the site occupancy. Now the XRD pattern of ICSD 67782 shows the octrahedral site for the mineral reported as the reference sample has a charge of 2.6 = x Fe + y Cu. Each site is assumed to be occupied so x+y =1, so 2.6 = 3*(1-y) + 2y. y= 0.4 x = 0.6. So ICSD reported mineral contained 40% Cu. The synthesised beaverite conjtained 32 % Cu

according to EDAX measurements which is somewhat less than that reported for the reference material. There may well be a correlation between the intensity of the ν_1 modes and the site occupancy of the Cu. If less than 40 % site occupancy the the expected symmetry is C_{2v} . With higher Cu concentrations the site symmetry would be C_s.

Raman and infrared spectra

The Raman spectrum of beaverite at 298 and 77K together with the infrared spectrum are shown in Figures 3, 4 and 5. Figure 3 displays the hydroxyl stretching region; Figure 4 the spectral region between 850 and 1350 cm^{-1}; Figure 5 the low wavenumber region. The results of the band component analyses are reported in Table 1. The infrared spectrum in the 2800 to 3600 cm^{-1} region is dominated by an intense broad band centred upon 3178 cm^{-1}. This band is attributed to a water stretching vibration. This band is not observed in the Raman spectra. In the infrared spectrum three additional bands are observed at 3446, 3346 and 3342 cm^{-1}. A likely attribution of these bands is to OH stretching vibrations associated with the OH units. Bands in similar positions are observed in the 298 K Raman spectrum at 3420, 3380 and 3354 cm^{-1}. These bands show a small shift upon collecting the spectra at 77 K. Multiple Raman OH stretching bands are indicative of non-equivalent OH units in the structure. Such non-equivalence will result from the substitution of Cu for Pb in the beaverite structure. Such information cannot be obtained from either single crystal XRD studies or from PXRD studies. Raman spectroscopy shows that the OH units are not exactly the same in the molecular structure of beaverite.

Sulphates as with other oxyanions lend themselves to analysis by Raman spectroscopy. In aqueous systems, the sulphate anion is of T_d symmetry and is characterised by Raman bands at 981 cm^{-1} (ν_1), 451 cm^{-1}(ν_2), 1104 cm^{-1} (ν_3) and 613 cm^{-1} (ν_4). Reduction in symmetry in the crystal structure of sulphates such as jarosites will cause the splitting of these vibrational modes. For jarosites the space group is C_5^3 and six sulphate fundamentals should be observed. The infrared spectrum of beaverite displays an intense broad band at 1004.3 cm^{-1} with a low intensity band also observed at 993.5 cm^{-1}. These bands are broad with bandwidths of 76.9 and 15.0 cm^{-1}. In the 298 K Raman spectrum three bands are observed at 1018.4, 1009.9 and 999.1 cm^{-1}. The bandwidths of 7.5, 21.0 and 8.8 cm^{-1} are found. Upon obtaining the spectra at 77 K three bands are resolved at 1019.8, 1011.6 and 1000.2 cm^{-1} with bandwidths of 6.9, 18.7 and 7.3 cm^{-1}. These infrared and Raman bands are attributed to the SO_4^{2-} symmetric stretching vibration. The non-equivalence of the sulphate units is brought about by the Cu substitution for Pb in the structure. The fact that multiple symmetric stretching vibrations are observed implies at least on the molecular scale, the non-equivalence of the sulphates in the structure. For natural K-jarosite three bands are observed at 1009.8, 1011.9 and 1026.3 cm^{-1} with bandwidths of 4.4, 6.1 and 11.5 cm^{-1}. These bands are likewise assigned to the (ν_1) SO_4^{2-} symmetric stretching mode. The observation of more than one band may be accounted for by the non-equivalence of the SO_4^{2-} units. A previous study by Sasaki et al. reported the band as a single band at 1006.7 cm^{-1} for a synthetic K-jarosite [23] which is in excellent agreement with this study. However the position of the band differs from that of the natural jarosite. For natural Na-jarosite the Raman spectrum shows an intense band at 1007.0 cm^{-1} with second band curve resolved at 1010.7 cm^{-1}. For plumbojarosite the Raman spectrum shows a single band at 1036 cm^{-1} attributed to the SO_4^{2-} symmetric stretching mode.

The equivalent infrared band is forbidden and is not observed. Sasaki reported the Raman bands for Pb-jarosite as 1107 and 1161 cm^{-1} in the Raman spectrum and 1080, 1092 and 1195 cm^{-1} in the infrared spectrum [23]. The spectrum of beaverite is subtly different from plumbojarosite (Figure 6). A band is observed in the infrared spectrum at 906 cm^{-1} which is not found in the Raman spectra. This band is attributed to the OH deformation mode.

In the infrared spectrum of beaverite two bands are observed at 1106.1 and 1077.3 cm^{-1}. In addition two bands are observed at 1191.7 and 1144.9 cm^{-1}. These bands may be assigned to the SO_4^{2-} antisymmetric stretching modes. It is suggested that there are two sets of SO_4^{2-} antisymmetric bands. In the Raman spectrum at 298 K, bands are curve resolved at 1175.5, 1163.9, 1116.5, 1102.7 and 1080.8 cm^{-1}. The bands in the 77 K spectrum are observed at 1177.6, 1154.9, 1109.6, 1106.4 and 1077.6 cm^{-1}. These bands are attributed to the SO_4^{2-} antisymmetric modes. The multiple vibrations in this spectral region are indicative of the non-equivalence of the sulphates in the beaverite structure. In comparison two Raman bands for plumbojarosite at 1099 and 1062 cm^{-1} are assigned to the SO_4^{2-} antisymmetric stretching modes. The two equivalent infrared bands for plumbojarosite are the two bands at 1182 and 1109 cm^{-1}. Sasaki et al. reported the Raman bands for Pb-jarosite as 1107 and 1161 cm^{-1} in the Raman spectrum and 1080, 1092 and 1195 cm^{-1} in the infrared spectrum [23].

The infrared spectrum of the low wavenumber region of beaverite shows two bands at 625.5 and 586.1 cm^{-1}. In the 298 K Raman spectrum bands are observed at 619.4, 576.5 and 560.4 cm^{-1}. In the 77 K spectrum bands are observed at 620.8, 579.1 and 552.5 cm^{-1}. These bands are attributed to the SO_4^{2-} ν_4 bending modes. The spectra of the K and Na jarosites in the low wavenumber region show bands at around 641, 625 and 575 cm^{-1}. The first two bands are ascribed to the ν_4 bending modes of the sulphate and the latter band may be assigned to a FeOH deformation mode. For plumbojarosite a band at 619 cm^{-1} in the infrared spectrum and at 674 cm^{-1} in the Raman spectrum is assigned to the ν_4 bending mode of the SO_4^{2-} units. The previous study which reported the Raman spectrum of Pb-jarosite gave two bands at 623 and 668 cm^{-1} in the infrared spectrum and at 623 cm^{-1} in the Raman spectrum [23].

The 298 K Raman spectrum shows an intense band at 441.0 cm^{-1} with a second intense band at 432.9 cm^{-1}. An additional band is observed at 455.8 cm^{-1}. In the 77 K spectrum bands are observed at 456.9, 441.9 and 414.0 cm^{-1}. These bands are ascribed to the SO_4^{2-} ν_2 bending modes. In the Raman spectrum of plumbojarosite two bands at 424 and 454 cm^{-1} are attributed to the ν_2 bending modes of the SO_4^{2-} units (Figure 7). K-jarosite shows two overlapping bands at 443.7 and 452.8 cm^{-1} with bandwidths of 12.0 and 10.7 cm^{-1} and are assigned to the ν_2 bending mode. The observation of two bands is simply due to symmetry lowering. The values differ considerably from that published for synthetic K-jarosite [23]. Sasaki et al. assigned the most intense band at 434.5 cm^{-1} to FeO stretching vibrations. Such an assignment is unlikely. The band is attributed to the ν_2 bending mode. Two bands are found at 354 to 365 cm^{-1} and at around 300 cm^{-1}. These bands are more likely due to FeO vibrations. For beaverite strong Raman bands are observed in the 298 K spectrum at 327.6 and 216.4 cm^{-1}; intense bands are observed in the 77 K spectrum at 300.3 and 220.8 cm^{-1}. The bands are sharp. These bands may be due to FeO stretching vibrations.

Conclusions

Minerals of the alunite supergroup which contains over forty mineral species all based upon the jarosite structure can be readily analysed using Raman spectroscopic techniques, even though X-ray diffraction patterns of these minerals may be difficult to obtain because of a lack of crystallinity. Raman spectroscopy is an important technique for the study of these types of sulphate minerals especially when the minerals may be non-crystalline making determination by X-ray diffraction techniques difficult.

Beaverite belongs to the jarosite mineral subgroup many of which contain sulphate and OH units which are readily detected by infrared and Raman spectroscopy. Naturally occurring beaverite contains approximately 40% Cu substitution and our synthessied compound contained 32 %. The spectra of beaverite show multiple bands for both the OH units and the SO_4^{2-} units, thus indicating the non-equivalence of the OH and sulphate units in the beaverite structure and the reduction of the symmetry of the sulphate in the beaverite structure to C_s. Such multiplicity is not as readily observed for plumbojarosite. The substitution of Cu^{2+} for Fe^{3+} in the beaverite structure makes the sulphate and OH units non-equivalent.

Acknowledgments

The financial and infra-structure support of the Queensland University of Technology Inorganic Materials Research Program of the School of Physical and Chemical Sciences is gratefully acknowledged. The Australian Research Council (ARC) is thanked for funding.

References

1. Dutrizac, JE, Jambor, JL. *Reviews in Mineralogy & Geochemistry* 2000**; 40**: 405.
2. Butler, BS, Schaller, WT. *Journal of the Washington Academy of Sciences* 1911**; 1**: 26.
3. Breidenstein, B, Schlueter, J, Gebhard, G. *Neues Jahrbuch fuer Mineralogie, Monatshefte* 1992: 213.
4. Jambor, JL, Dutrizac, JE. *Canadian Mineralogist* 1983**; 21**: 101.
5. Hilebranad, WF, Wright, FE. *American Journal of Science* 1910**; 30**: 191.
6. Leach, FI. *Mining Journal (Phoenix)* 1937**; 20**: 40.
7. Mumme, WG, Scott, TR. *American Mineralogist* 1966**; 51**: 443.
8. Dutrizac, JE, Dinardo, O, Kaiman, S. *Hydrometallurgy* 1980**; 5**: 305.
9. Taberdar, T, Gulensoy, H, Aydin, AO. *Marmara Universitesi Fen Bilimleri Dergisi* 1985**; 2**: 76.
10. Amoros, JL, Lunar, R, Tavira, P. *Mineralium Deposita* 1981**; 16**: 205.
11. Rewitzer, C, Hochleitner, R. *Rivista Mineralogica Italiana* 1989: 83.
12. Harris, DL, Lottermoser, BG, Duchesne, J. *Australian Journal of Earth Sciences* 2003**; 50**: 797.
13. Hudson-Edwards, KA, Schell, C, Macklin, MG. *Applied Geochemistry* 1999**; 14**: 1015.
14. Buckby, T, Black, S, Coleman, ML, Hodson, ME. *Mineralogical Magazine* 2003**; 67**: 263.
15. Williams, PA *Oxide Zone Geochemistry*; Ellis Horwood Ltd, Chichester, West Sussex, England, 1990.
16. Drouet, C, Navrotsky, A. *Geochimica et Cosmochimica Acta* 2003**; 67**: 2063.
17. Adler, HH, Kerr, PF. *American Mineralogist* 1965**; 50**: 132.
18. Serna, CJ, Parada Cortina, C, Garcia Ramos, JV. *Spectrochimica Acta, Part A: Molecular and Biomolecular Spectroscopy* 1986**; 42A**: 729.
19. Sasaki, K. *Canadian Mineralogist* 1997**; 35**: 999.
20. Omori, K, Kerr, PF. *Geological Society of America Bulletin* 1963**; 74**: 709.
21. Hunt, GR. *Geophysics* 1979**; 44**: 1974.
22. Arkhipenko, DK, Devyatkina, ET, Pal'chik, NA. *Kristallokhimiya i Rentgenogr. Mineralov, L.* 1987: 138.
23. Sasaki, K, Tanaike, O, Konno, H. *Canadian Mineralogist* 1998**; 36**: 1225.
24. Jambor, JL, Dutrizac, JE. *Canadian Mineralogist* 1985**; 23**: 47.

Table 1 Table of the infrared and Raman spectra of synthetic beaverite

Infrared			Raman at 298 K			Raman at 77 K		
Centre	FWHM	% Area	**Centre**	FWHM	% Area	**Centre**	FWHM	% Area
3446.0	88.7	0.4						
			3420.9	121.1	5.6	**3424.7**	102.3	3.3
						3386.3	164.8	10.5
			3380.1	29.7	0.4	**3380.4**	18.9	0.4
3346.1	24.7	0.2	**3354.4**	229.8	8.5			
3342.6	161.2	4.8						
3178.1	297.5	6.9						
						1319.3	50.2	0.9
						1258.7	145.3	2.0
1239.4	21.2	0.5						
1191.7	52.4	5.0						
			1175.7	26.1	2.2	**1177.6**	12.2	0.3
			1163.9	109.8	4.1	**1170.6**	30.9	3.3
1144.9	49.9	2.3	**1156.3**	17.4	0.8	**1154.9**	14.9	0.4
			1116.5	26.8	2.3	**1109.6**	32.4	7.1
1106.1	30.8	3.5	**1102.7**	19.9	11.2	**1106.4**	14.2	3.8
			1080.8	78.1	3.7			
1077.3	28.4	4.6	**1076.3**	15.6	0.9	**1077.6**	11.5	0.3
						1069.0	48.8	1.1
			1018.4	7.5	0.5	**1019.8**	6.9	0.8
1004.3	76.9	19.3	**1009.9**	21.0	6.8	**1011.6**	18.7	4.6
993.5	15.0	0.6	**999.1**	8.8	3.5	**1000.2**	7.3	2.2
900.0	70.9	7.9						
790.3	45.4	6.3						
						703.3	60.0	1.0
689.2	225.8	14.6						
671.4	16.2	0.1						
			645.2	21.8	0.6	**651.2**	42.1	0.8
625.5	30.6	2.5	**624.3**	15.8	1.0			
			619.4	10.4	2.2	**620.8**	10.4	2.1
586.1	39.0	6.4				**594.2**	145.8	4.1
			576.5	16.5	1.2	**579.1**	16.1	0.9
			560.4	74.5	7.2	**552.5**	28.6	1.3
511.9	321.3	14.0						
			480.5	39.8	2.8	**482.4**	28.8	3.8
			455.8	11.9	1.2	**456.9**	9.1	0.4
			441.0	18.8	5.8	**441.9**	15.5	5.8
			432.9	50.9	2.3			
						414.0	101.5	18.4
			391.5	39.2	1.3	**399.3**	15.7	1.2
						386.4	17.4	3.7
			356.3	26.4	0.7	**357.2**	11.3	0.1
			335.4	18.1	0.9	**338.5**	16.2	1.1
			327.6	44.2	5.4			
			298.4	10.6	0.4	**300.3**	9.1	1.1
						295.9	14.2	1.5
			278.0	38.7	2.3	**282.4**	90.4	5.2
			258.5	19.6	2.2	**260.2**	11.6	0.4
			242.0	30.0	3.3	**245.4**	18.2	1.0
			216.4	18.1	4.4	**220.8**	18.3	3.8
			201.8	22.1	4.1	**201.4**	15.6	0.8
			172.5	9.8	0.2	**184.4**	34.0	0.6

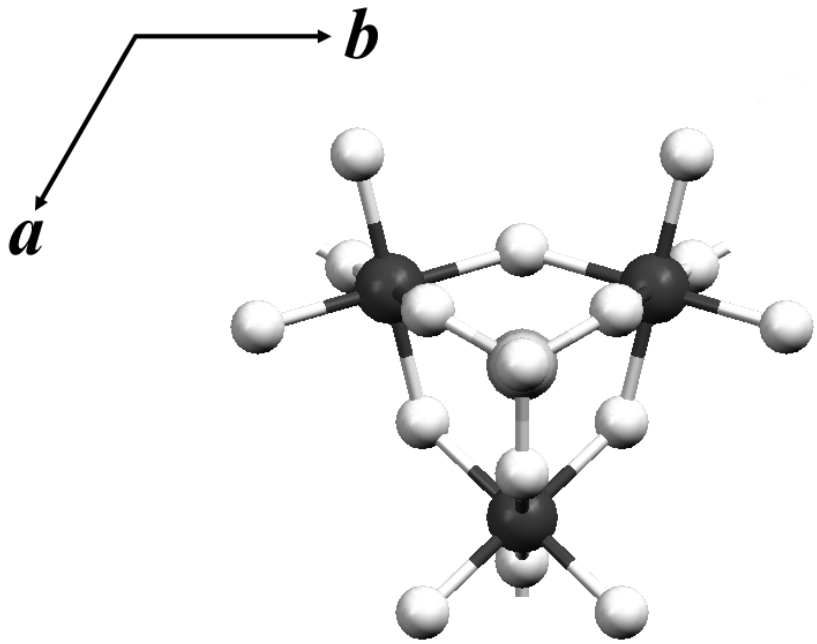

Figure 1

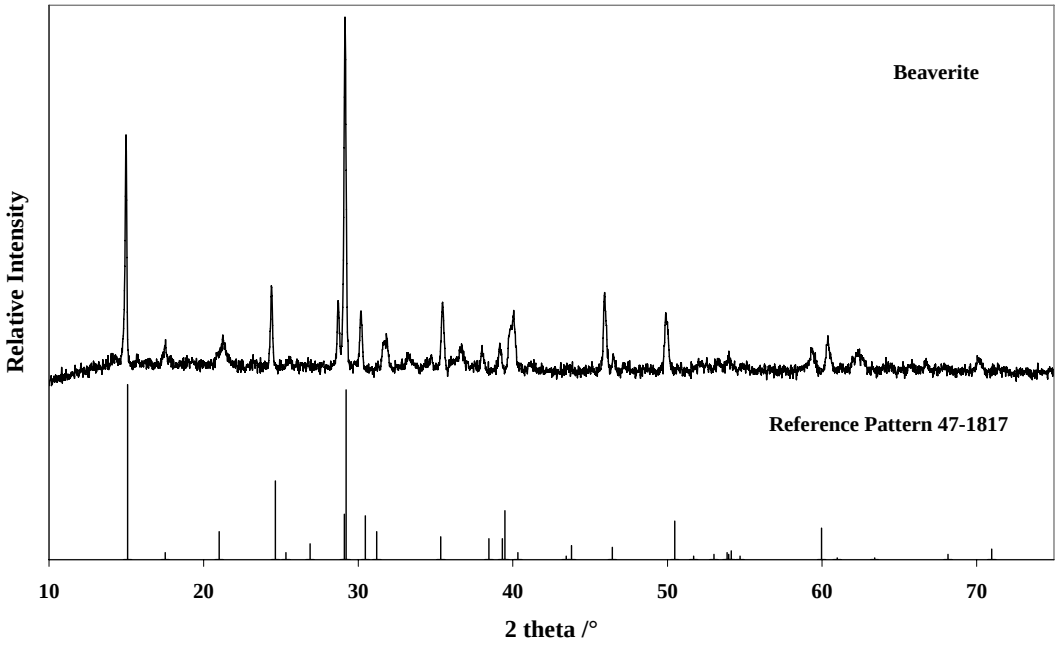

Figure 2

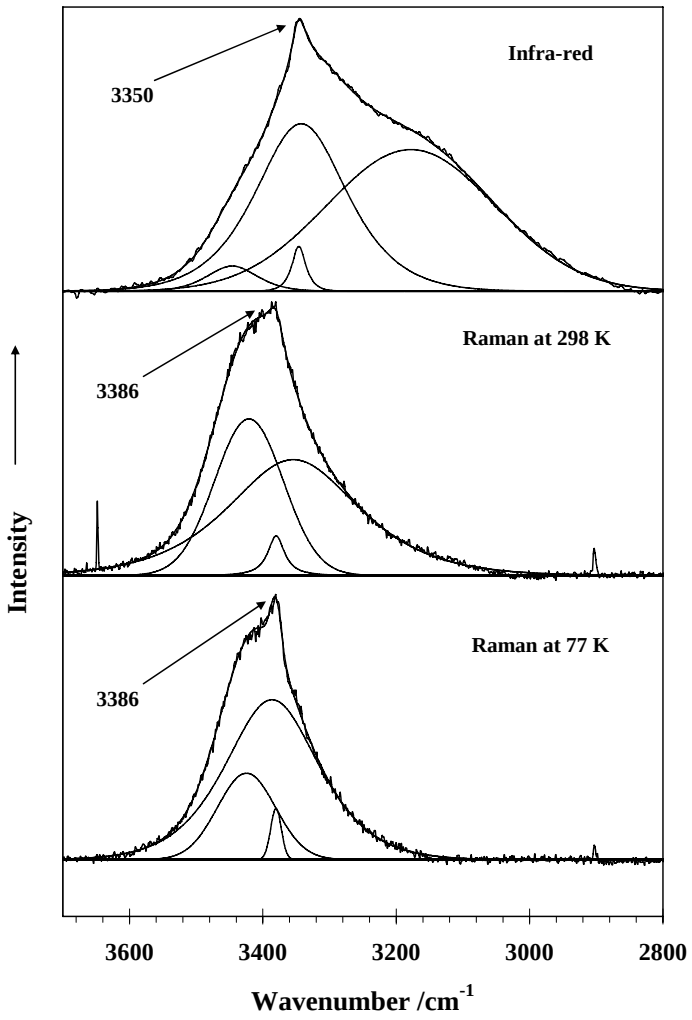
Infra-red
3350
Raman at 298 K
3386
Raman at 77 K
3386
Intensity
3600
3400
3200
3000
2800
Wavenumber /cm-1

Figure 3

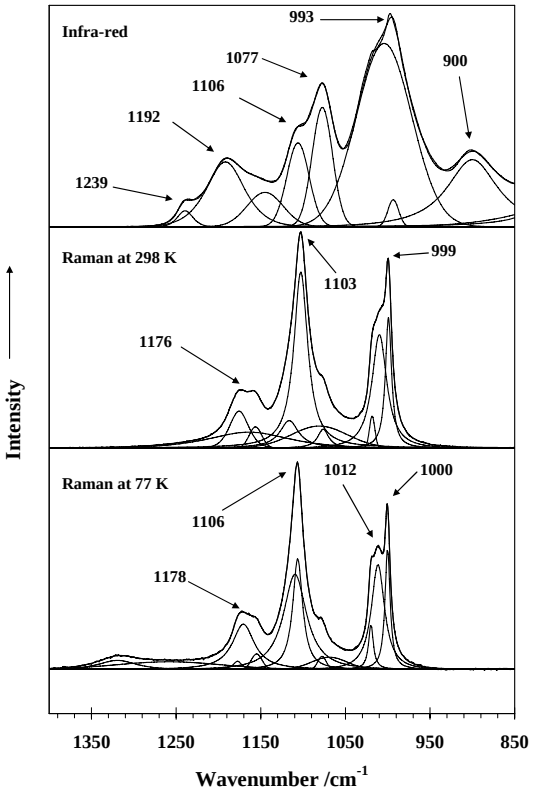

Figure 4

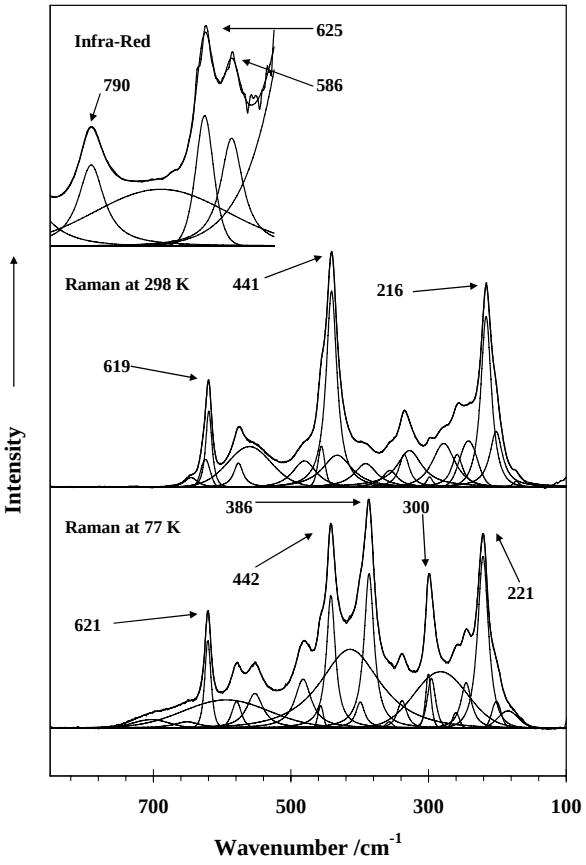

Figure 5

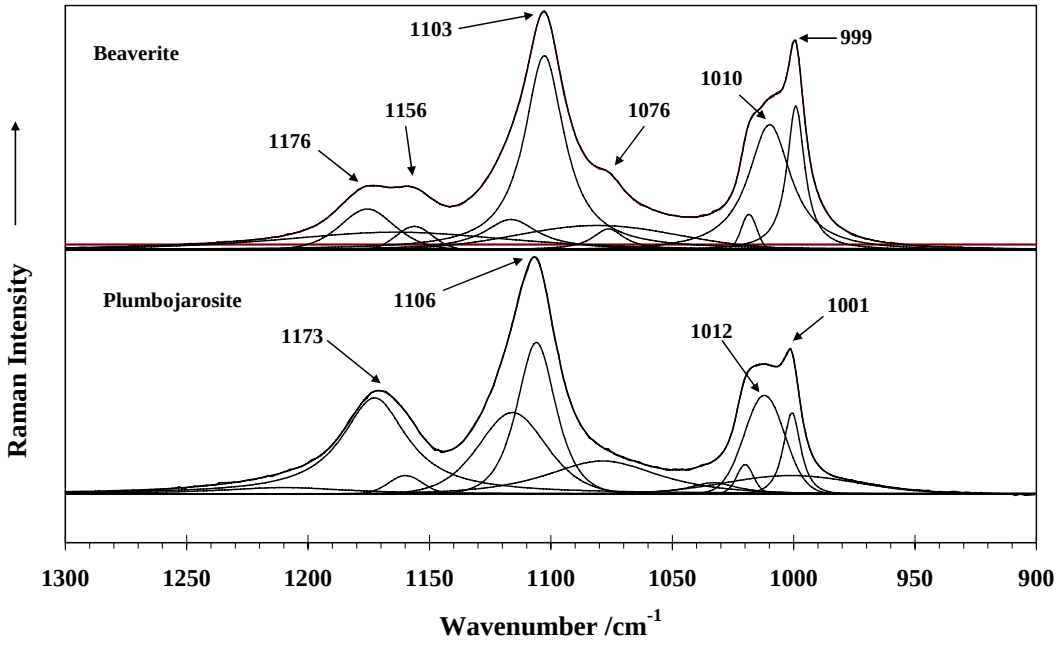

Figure 6

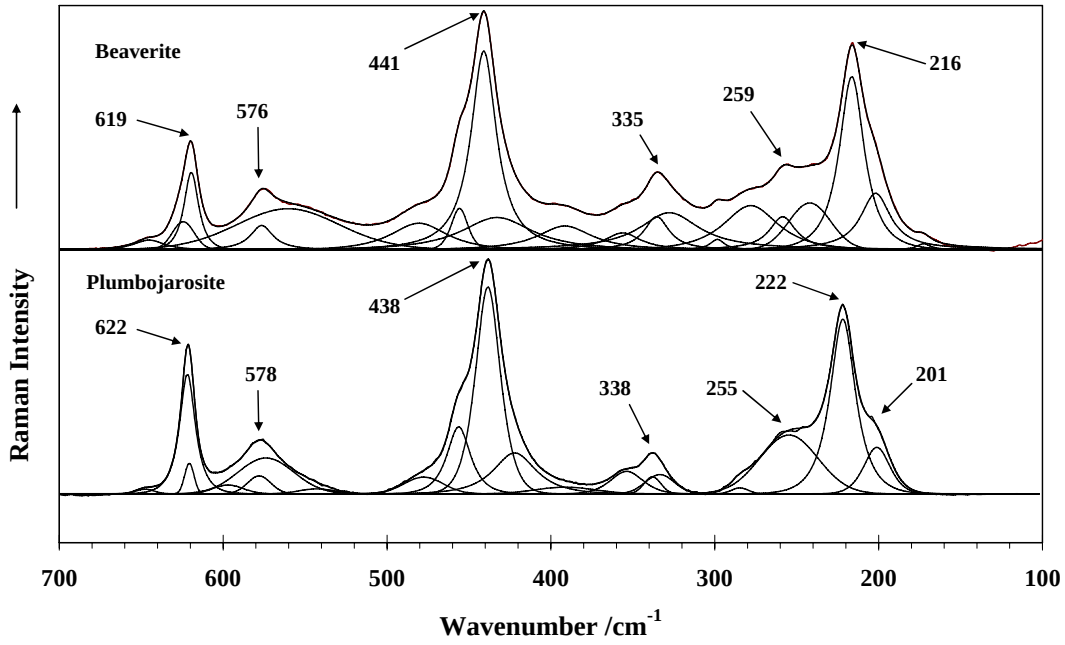

Figure 7

List of Figures